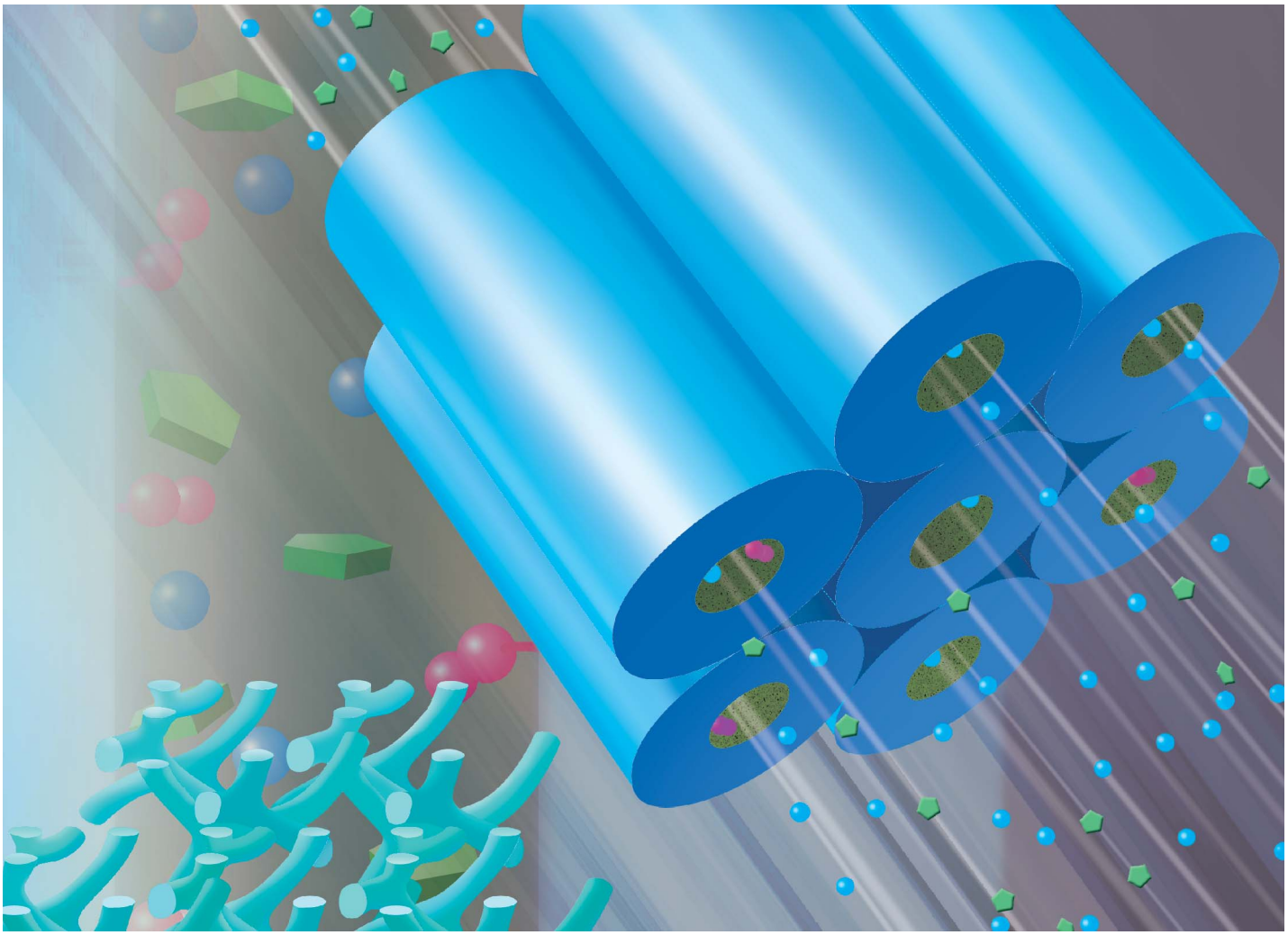

Showcasing liquid crystal research from groups at the Department of Chemistry and Biotechnology, the University of Tokyo, CREST, JST, and the Department of Biotechnology, Tokyo University of Agriculture and Technology, Japan.

Title: Zwitterionic liquid crystals as 1D and 3D lithium ion transport media

Zwitterionic liquid crystals forming nanosegregated columnar and bicontinuous cubic phases are used as media for the transport of lithium ions within the well-defined ionic nanochannels. Enhanced conductivities are achieved for multicomponent systems including a zwitterionic liquid crystal, a lithium salt and propylene carbonate.

As featured in:

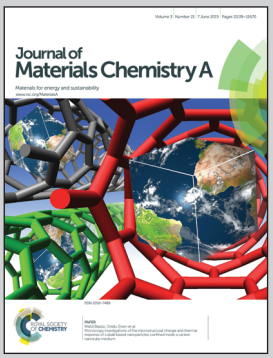

See Masafumi Yoshio, Takashi Kato *et al.*, *J. Mater. Chem. A*, 2015, **3**, 11232.

ROYAL SOCIETY OF CHEMISTRY

www.rsc.org/MaterialsA

Registered charity number: 207890

Journal of Materials Chemistry A

PAPER

View Article Online
View Journal | View Issue

Cite this: J. Mater. Chem. A, 2015, 3, 11232

Zwitterionic liquid crystals as 1D and 3D lithium ion transport media†

Bartolome Soberats,[ab] Masafumi Yoshio,*[a] Takahiro Ichikawa,[c] Hiroyuki Ohno[c] and Takashi Kato*[ab]

Received 31st January 2015
Accepted 19th March 2015

DOI: 10.1039/c5ta00814j

www.rsc.org/MaterialsA

We describe the development of self-assembled one- and three-dimensional lithium ion conductors composed of zwitterionic liquid crystals, lithium bis(trifluoromethylsulfonyl)imide (**LiTFSI**) and propylene carbonate (**PC**). Two types of wedge-shaped zwitterions based on imidazolium dicyanoethenolate and sulfonate were synthesized. These compounds alone show liquid-crystalline (LC) columnar hexagonal (Col_h) phases and low ionic conductivities (10^{-8} to 10^{-7} S cm^{-1}). The increase in the ionic conductivities was achieved by the addition of **LiTFSI** (10^{-5} S cm^{-1}) followed by that of **PC** (10^{-4} S cm^{-1}). Moreover, LC bicontinuous cubic (Cub_{bi}) phases are induced by tuning the ionic nature of the zwitterionic liquid crystal with the ratio of **LiTFSI** and **PC**. The dissociation of **LiTFSI** in the zwitterions and the ion–dipole interaction between the lithium ions and **PC** are shown to be significant keys for the enhancement of the conductivities and stabilization of the nanosegregated LC structures.

Introduction

The construction of supramolecular nanostructures with diverse functionalities using molecular self-assembly is of increasing interest for emerging nanotechnologies.[1–19] An important challenge is to build nanochannels capable of ion transport.[20–44] The use of liquid-crystalline (LC) self-assembly is a promising approach for the development of nanochannels with various dimensions and enhanced ion transport function.[20,30–46] Recently, LC ion-conductive materials have been applied to energy devices, such as lithium ion batteries and dye-sensitized solar cells.[47–50] Among the LC organizations, thermotropic LC bicontinuous cubic (Cub_{bi}) assemblies have attracted considerable attention because they form three-dimensionally interconnected ionic channels suitable for ion transport.[34,38,44–46] However, the design of three-dimensional (3D) ion-conductive thermotropic LC materials is still challenging because the formation of Cub_{bi} phases requires a delicate balance of volume and interactions between the polar and the non-polar parts in the material.[44] One of the approaches for the induction of functional thermotropic Cub_{bi} phases is the use of two-component assemblies.[51–54] For example, we achieved 3D proton transport in the Cub_{bi} phases formed by the complexation of zwitterionic molecules and organic acids.[52,53] The acid dissociates in the presence of zwitterions, which enables the proton transport. Interestingly, the proton conductivity and LC behavior are tuned by the amount of acid and also by the further addition of water.[53] LC Cub_{bi} phases were also induced for the complexes of pyridinium-based zwitterions and lithium salts, although their ionic conductivities were not examined.[54] Anhydrous 3D lithium ion transport was previously achieved in LC materials by mixing lithium salts and ionic molecules.[31,55] For example, we developed nanostructured polymer electrolytes upon photo-crosslinking of thermotropic LC Cub_{bi} assemblies composed of wedge-shaped ammonium salts and a lithium salt.[55] Gin and co-workers also reported LC Cub_{bi} polymer electrolytes based on the lyotropic LC assemblies of a polymerizable lithium sulfonate and a dilute $LiClO_4$ solution in propylene carbonate (**PC**).[31] These approaches are based on the solubilization of lithium ions in nanostructured channels. However, we consider that the dissociation of lithium salts in zwitterionic LC media is a promising strategy for the development of lithium ion transport materials with induced Cub_{bi} phases.

Herein we report on the development of one-dimensional (1D) and 3D lithium ion transport channels (Fig. 1). We designed and prepared imidazolium-type zwitterions **1** and **2** (Fig. 2) to co-assemble with lithium bis(trifluoromethylsulfonyl) imide (**LiTFSI**) and **PC** forming well-defined ionic pathways capable of lithium transport (Fig. 1 and 2). Our approach and material design in the present study is to use zwitterionic liquid

[a]Department of Chemistry and Biotechnology, School of Engineering, The University of Tokyo, Hongo, Bunkyo-ku, Tokyo 113-8656, Japan. E-mail: yoshio@chembio.t.u-tokyo.ac.jp; kato@chiral.t.u-tokyo.ac.jp

[b]CREST, JST, 4-1-8, Honcho, Kawaguchi, Saitama, 332-0012, Japan

[c]Department of Biotechnology, Tokyo University of Agriculture and Technology, Nakacho, Koganei, Tokyo 184-8588, Japan

† Electronic supplementary information (ESI) available: Materials and methods, synthetic procedures, characterization of compounds, thermogravimetric analyses of the materials, liquid crystalline characterization experiments including XRD patterns and POM images, ^{7}Li NMR studies, IR spectra and supplementary ion conduction measurements. See DOI: 10.1039/c5ta00814j

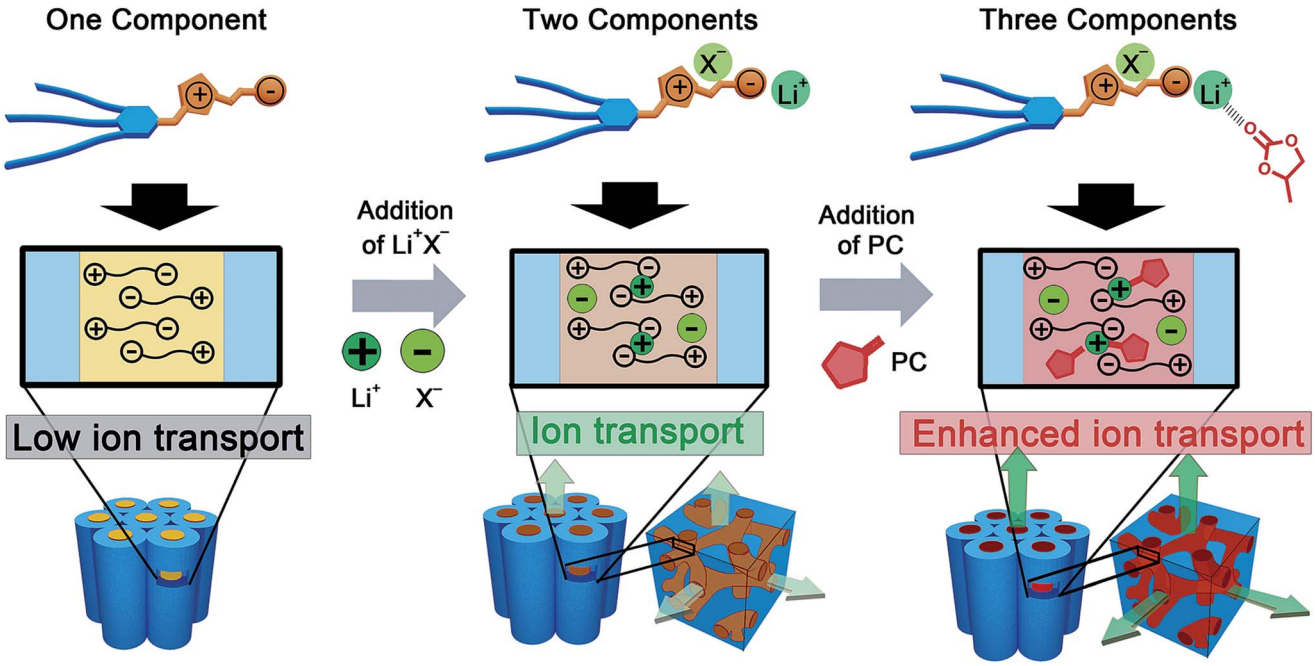

Fig. 1 Our design strategy for the enhancement of lithium ion transport based on three components of nanostructured liquid-crystalline (LC) materials formed by the self-assembly of a zwitterionic liquid crystal, a lithium salt and propylene carbonate (**PC**). Green arrows indicate the direction of ion transport. The ionic channels are shown in yellow, orange, or red colors depending on their composition and the aliphatic parts are indicated in blue. The proposed organizations of molecules and salt inside the ionic channels are shown in the zoom windows from side views.

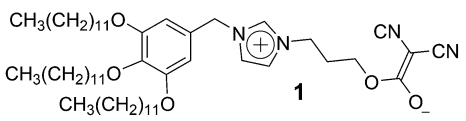

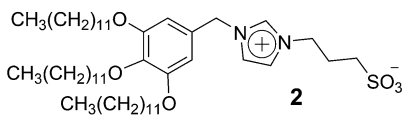

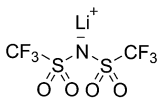

LiTFSI

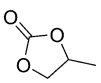

PC

Fig. 2 Chemical structures of the LC zwitterions **1** and **2**, lithium bis(trifluoromethylsulfonyl)imide (**LiTFSI**) and **PC**.

crystals as media for lithium ion transport. Zwitterionic liquid crystals tethering charge-delocalized anions are expected to form well-defined ionic channels, but have no transportable ions (Fig. 1, left). After the addition of a lithium salt, the salt may be dissociated by the interactions with zwitterionic moieties, which allows lithium to move along the ionic pathways (Fig. 1, middle). At the same time, our intention is to increase the lithium ion mobility by incorporating **PC** as a polar additive (Fig. 1, right).[31] It is expected that the optimization of the ratio of additives, lithium salt and **PC**, can induce Cub_{bi} phases and enhance the ionic conductivities (Fig. 1).

Results and discussion

Material design

Wedge-shaped zwitterions **1** and **2** (Fig. 2) are designed to act as LC ion transport media. The ionic parts of **1** and **2** consist of an imidazolium moiety tethering a dicyanoethenolate anion[56–59] or a sulfonate anion[52–54,60] through a propylene spacer. We expected that compounds **1** and **2** would show different LC phase transition behavior and ion transport properties due to the differences in the size of the anions and in the distribution of negative charges. **LiTFSI** (Fig. 2) is chosen as a lithium ion source because of its thermal stability and high delocalization of negative charges.[35,54,61] Ohno and co-workers previously reported that the equimolar mixtures of imidazolium-based sulfobetaine whose melting point is over 100 °C and lithium salts (**LiTFSI**, $LiOSO_2CF_3$, $LiBF_4$, and $LiClO_4$) become ionic liquids at room temperature.[62] Among them, the **LiTFSI** complex exhibits the lowest glass transition temperature and the highest ionic conductivity.[62] Lin and co-workers reported that the mixtures of imidazolium-type carboxylates or sulfonates and **LiTFSI** form smectic A phases exhibiting ionic conductivities.[63,64] In addition, the employment of bulky **LiTFSI** as an additive for zwitterionic liquid crystals can induce structural changes of LC phases because of the change of the molecular shapes and the volume balance between the polar and nonpolar parts.[35,54] Thus we considered that the

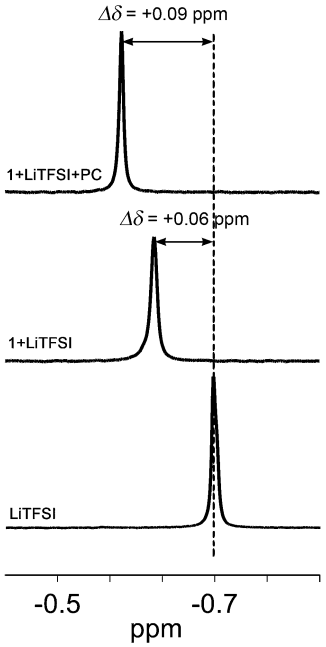

Fig. 3 ^{7}Li NMR spectra of **LiTFSI** (0.013 m, 450 μl) (bottom), **1**/**LiTFSI** (0.02 m/0.013 m, 450 μl) (middle) and **1**/**LiTFSI**/**PC** (0.02 m/0.013 m/0.13 m, 450 μl) (top) in $CDCl_3$: THF-d_6 (v/v, 6 : 1) solution. LiCl D_2O solution in a coaxial NMR tube was used as an internal standard and the lithium signal was set at 0 ppm. The dashed line indicates the chemical shift of the lithium ion for the pure **LiTFSI** solution. All the spectra were recorded at room temperature.

Table 1 LC behavior of zwitterionic compounds and their mixtures with **LiTFSI** and/or **PC**

Sample[a]	Phase transition behavior[b]				
1			Col_h	217	Decomp.
1/Li^+(20)			Col_h	190	Decomp.
1/Li^+(50)	Cub_{bi}	65–88	Col_h	190	Decomp.
1/Li^+(20)**PC**(5)	Cub_{bi}	50–68	Col_h	120[c]	
1/Li^+(20)**PC**(10)	Cub_{bi}	50–75	Col_h	120[c]	
1/Li^+(50)**PC**(5)	Cub_{bi}	81–92			Iso
1/Li^+(50)**PC**(10)	Cub_{bi}	74–86			Iso
2			Col_h	207	Decomp.
2/Li^+(20)			Col_h	200	Decomp.
2/Li^+(50)			Col_h	200	Decomp.
2/Li^+(20)**PC**(5)			Col_h	120[c]	
2/Li^+(20)**PC**(10)			Col_h	120[c]	
2/Li^+(50)**PC**(5)			Col_h	120[c]	
2/Li^+(50)**PC**(10)			Col_h	120[c]	

[a] Ratio of **LiTFSI** and **PC** is indicated as follows: **1**/Li^+(x), **2**/Li^+(x), **1**/Li^+(x)**PC**(y) and **2**/Li^+(x)**PC**(y), where x is the mol% of **LiTFSI** and y indicates the wt% of **PC**. [b] Determined by polarizing optical microscope observation. The LC behavior was examined on heating processes (5 °C min^{-1}) from 25 °C to decomposition or isotropization temperature of the sample. The given transition temperatures correspond to the starting of the phase transitions. In the case of a slow phase transition, a temperature range is given. Mixtures containing more than 50 mol% of **LiTFSI** show no homogeneous LC phases. Mixtures with 15 wt% or more of **PC** showed biphasic behavior. [c] For **PC** containing samples, the microscopic observation was conducted up to 120 °C. All the mixtures showed decomposition at around 200 °C. Col_h: columnar hexagonal, Cub_{bi}: bicontinuous cubic, Iso: isotropic, and Decomp.: decomposition.

complexation of **1** or **2** and **LiTFSI** would lead to the development of 3D lithium ion conductive materials exhibiting Cub_{bi} LC phases. Furthermore, to enhance the dissociation of lithium ions in the zwitterionic ion transport media, **PC** (Fig. 2) is used as a polar additive because the carbonyl group of **PC** has the ability to coordinate to lithium ions.[31,40,48,61]

Supramolecular interactions between components

In order to examine the interactions between lithium ions, zwitterions and **PC**, ^{7}Li NMR measurements of **LiTFSI**, the mixture of **1** and **LiTFSI** and the tertiary mixture of **LiTFSI**, **1** and **PC** were conducted in the $CDCl_3$/THF-d_6 solutions using LiCl in D_2O as an internal standard (Fig. 3). The results for **2** are shown in the ESI (Fig. S10†). The ^{7}Li chemical shift of **LiTFSI** shows a downfield shift of 0.06 ppm in the presence of **1** (Fig. 3, middle). This result suggests the formation of a complex between **1** and **LiTFSI**, where the lithium ion may interact with the dicyanoethenolate anion (Fig. 1, top middle and Fig. S9†).[65,66] The addition of **PC** to the mixture of **1** and **LiTFSI** induces a further downfield shift of 0.03 ppm (Fig. 3, top) compared to the chemical shift for the mixture of **1** and **LiTFSI** (Fig. 3, middle). This shift may be attributed to the ion–dipole interactions between lithium ions and **PC**. It should be mentioned that the stepwise downfield shifts of the ^{7}Li signal are detected by the addition of zwitterions followed by **PC**, in spite of the presence of THF which is a competitive solvent.

The interactions between **1**, **LiTFSI** and **PC** were also confirmed by IR measurements in the bulk state. The IR spectra of **1**, the mixture of **1** and **LiTFSI** and the tertiary mixture of **1**, **LiTFSI** and **PC** were recorded at room temperature (Fig. S11†). Single compound **1** shows two absorption bands at 2193 and

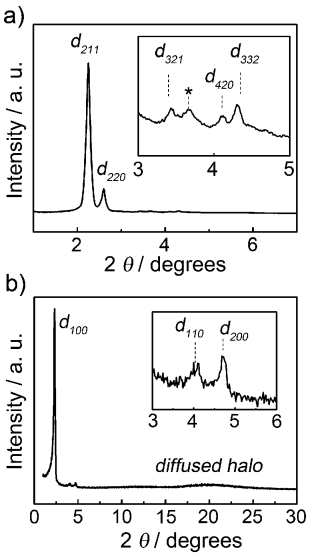

Fig. 4 X-ray diffraction (XRD) patterns of **1**/Li^+(50) at (a) 55 °C and (b) 120 °C. The mark * corresponds to the diffraction of the Kapton® film.

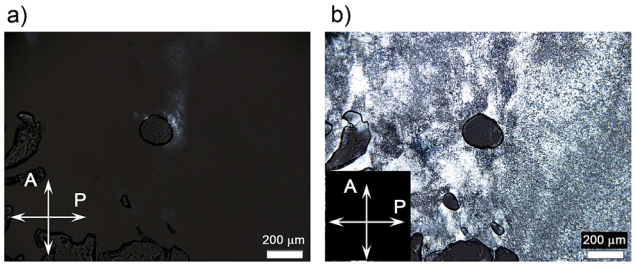

Fig. 5 Polarizing optical microscopy (POM) images of **1**/Li$^+$(50) at (a) 58 °C and (b) 90 °C. a: analyzer; p: polarizer.

2165 cm^{-1} which are characteristic of the C≡N vibrations of the dicyanoethenolate moiety.[57] These bands are shifted to 2202 and 2173 cm^{-1}, respectively, after the addition of 50 mol% of **LiTFSI**. Further addition of 10 wt% of **PC** resulted in a high wavenumber shift of CN bands to 2206 and 2179 cm^{-1}, respectively. These results suggest the existence of interactions between the zwitterionic molecule, **LiTFSI** and **PC**.

Liquid-crystalline properties

Compounds **1** and **2** show LC columnar hexagonal (Col_h) phases from room temperature to around 200 °C at which decomposition occurs (Table 1 and S1†). Mixtures of the zwitterions with **LiTFSI** [**1**/Li$^+$(x) and **2**/Li$^+$(x), x denotes the mol% of **LiTFSI**] were prepared by mixing the THF solutions of **LiTFSI** and the zwitterions, followed by the evaporation of the solvent to yield the anhydrous mixtures as white solids. The liquid crystallinity of the **1**/Li$^+$(x) and **2**/Li$^+$(x) mixtures was examined by polarizing optical microscopy (POM), X-ray diffraction (XRD) and differential scanning calorimetry. The **1**/Li$^+$(x) mixtures with 10–40 mol% of **LiTFSI** and all the **2**/Li$^+$(x) mixtures exhibit only Col_h phases (Table 1 and S1†).‡ As for **1**/Li$^+$(50), the Cub_{bi} phase is induced in addition to the formation of the Col_h phase. The Cub_{bi} phase is observed from room temperature to 65 °C and slowly changes to the Col_h phase between 65 and 88 °C under POM observation at the heating rate of 5 °C min^{-1}. The formation of ionic pairs composed of ionic liquid-like imidazolium TFSI and lithium dicyanoethenolate, which is bulkier than lithium sulfonate, may disturb the columnar packing.[59] The change in the volume fraction of the polar and nonpolar parts may also contribute to the induction of the Cub_{bi} phase.[51–54] Fig. 4 and 5 show the XRD patterns and POM images of **1**/Li$^+$(50) in the Cub_{bi} and Col_h phases. The small-angle XRD pattern of **1**/Li$^+$(50) at 55 °C (Fig. 4a) shows two strong and three weak peaks at 39.2, 34.0, 25.7, 21.4 and 20.4 Å corresponding to the (211), (220), (321), (420) and (332) reflections, respectively. The reciprocal d-spacing ratio of these peaks is $\sqrt{6} : \sqrt{8} : \sqrt{14} : \sqrt{20} : \sqrt{22}$, which corresponds to a Cub_{bi} phase with an $Ia3d$ symmetry. In contrast, the wide-angle XRD pattern of **1**/Li$^+$(50) at 120 °C (Fig. 4b) shows the (100), (110) and (200) reflections, which are characteristic of a Col_h phase. The POM image of **1**/Li$^+$(50) at 58 °C shows no birefringence (Fig. 5a), indicating the formation of a Cub_{bi} phase. By heating the sample to 90 °C (Fig. 5b), a birefringence upon the formation of the Col_h phase with polydomain organization is observed.

Compounds **1** and **2** and the mixtures **1**/Li$^+$(20), **1**/Li$^+$(50), **2**/Li$^+$(20) and **2**/Li$^+$(50) were selected to study the effects of the addition of **PC**. Compounds **1** and **2** show biphasic behavior after the addition of 5 and 10 wt% of **PC**.§ In contrast, the mixtures **1**/Li$^+$(x) and **2**/Li$^+$(x) form homogenous LC mixtures upon the addition of 5 or 10 wt% of **PC** [**1**/Li$^+$(x)**PC**(y) and **2**/Li$^+$(x)**PC**(y), y indicates the wt% of **PC**] (Table 1).¶ These results suggest that **LiTFSI** is essential for the stabilization of the LC phases in the mixtures containing zwitterions **1** or **2** and **PC**. The mixtures of **2**/Li$^+$(x)**PC**(y) show only Col_h phases, but the mixtures based on **1**/Li$^+$(x)**PC**(y) exhibit Cub_{bi} LC phases (Table 1). This behavior also indicates that the interactions of

‡ Mixtures containing more than 50 mol% of **LiTFSI** show no homogeneous LC phases.

Table 2 Lattice parameters of the LC phases determined by XRD measurements

Sample	Lattice parameters (Å)	LC phase[a]	Temperature (°C)
1	40.8	Col_h	120
1/Li$^+$(50)	43.4	Col_h	120
1/Li$^+$(50)	96.1	Cub_{bi}	55
1/Li$^+$(50)**PC**(10)	98.7	Cub_{bi}	60
2	40.4	Col_h	100
2/Li$^+$(50)	41.3	Col_h	100
2/Li$^+$(50)**PC**(10)	42.2	Col_h	100

[a] Col_h: columnar hexagonal; Cub_{bi}: bicontinuous cubic.

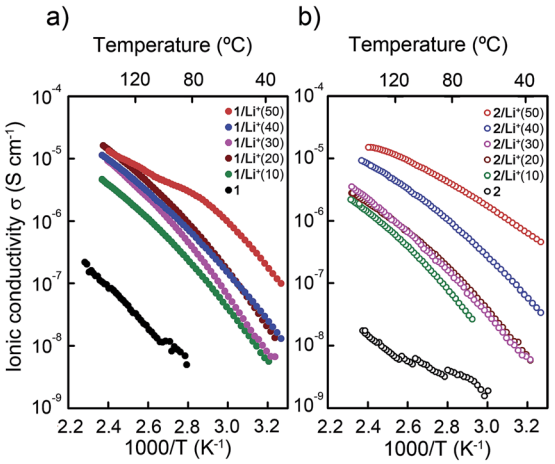

Fig. 6 Ionic conductivities as a function of temperature of (a) **1** and the mixtures **1**/Li$^+$(x) and (b) **2** and the mixtures **2**/Li$^+$(x). x indicates the mol% of LiTFSI.

§ The wt% of **PC** is given with respect to the mass of the zwitterion. 5 and 10 wt% of **PC** is roughly equivalent to 22 and 45 mol% of **PC** with respect to the zwitterion.

¶ Mixtures **1**/Li$^+$(x) and **2**/Li$^+$(x) show biphasic behaviour after the addition of 15 wt% or more of **PC**. Microscopy images of a mixture exhibiting biphasic behavior are shown in Fig. S2.

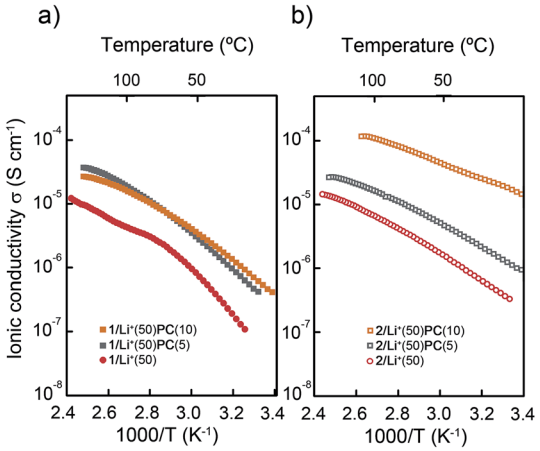

Fig. 7 Ionic conductivities as a function of temperature for the mixtures; (a) **1**/Li$^+$(50)**PC**(*y*) and (b) **2**/Li$^+$(50)**PC**(*y*). *y* denotes the wt% of **PC**.

dicyanoethenolate anions, lithium ions and **PC** play key roles in the induction of cubic phases. For example, **1**/Li$^+$(20) shows only a Col$_h$ phase, but Cub$_{bi}$ phases are formed after the addition of 5 or 10 wt% of **PC** (Table 1). Moreover, the cubic phase observed for **1**/Li$^+$(50) is thermally stabilized up to 80 °C by adding **PC** (Table 1). Remarkably, as far as we know the use of **PC** for the induction or stabilization of Cub$_{bi}$ phases has not yet been reported.

In order to obtain more details about the structural organization of these complexes, we studied the XRD parameters of the LC phases of **1**, **2**, and the selected mixtures with **LiTFSI** and **LiTFSI**/**PC**. Table 2 displays the unit cell distances for the Cub$_{bi}$ phases and the intercolumnar distances for the Col$_h$ phases of the selected mixtures. Compounds **1** and **2** in the Col$_h$ phases show intercolumnar distances of 40 Å. The molecular lengths of **1** and **2** in the extended conformation are estimated to be 33 and 30 Å, respectively. Thus, these results suggest that these zwitterionic molecules self-assemble into well-packed Col$_h$ structures, where aliphatic chains and zwitterionic moieties are interdigitated (Fig. 1 and S9†).[51–54,60,63,64] The addition of 50 mol% of **LiTFSI** to **1** and **2** leads to an increase in the intercolumnar distances (Table 2). In the case of **2**/Li$^+$(50), the intercolumnar distance also increases upon the addition of 10 wt% of **PC**. A similar increase is observed in the Cub$_{bi}$ phases of **1**/Li$^+$(50) after the addition of 10 wt% of **PC**, where the unit cell distance increases by 2.6 Å (Table 2). These results imply that **LiTFSI** and **PC** are incorporated within the ionic channels by interacting with the zwitterionic moieties (Fig. 1, S8, S9 and S11†).

Ionic conductivities

The ionic conductivities of the zwitterions **1** and **2**, and the mixtures **1**/Li$^+$(*x*), **2**/Li$^+$(*x*), **1**/Li$^+$(*x*)**PC**(*y*) and **2**/Li$^+$(*x*)**PC**(*y*) were measured as a function of temperature (Fig. 6, 7 and S12†) by the alternating current impedance method.[33] All the conductivities were measured using heating processes. Fig. 6 shows the ionic conductivities of the mixtures based on **1** (Fig. 6a) and **2** (6b) containing 0 to 50 mol% of **LiTFSI**. All samples are not aligned. The samples exhibiting the Col$_h$ phases show polydomain textures under POM observation (Fig. 5b). The addition of **LiTFSI** to **1** and **2** significantly increases the ionic conductivities. This observation suggests that the presence of mobile species enhances the ionic conductivities in the systems. The ionic conductivities for **1**/Li$^+$(*x*) and **2**/Li$^+$(*x*) increase with increasing amounts of **LiTFSI**. This enhancement is more significant for the **2**/Li$^+$(*x*) mixtures than that for the **1**/Li$^+$(*x*) mixtures. For example, the value of the ionic conductivity of **2** at 100 °C is 5×10^{-9} S cm^{-1} while the **2**/Li$^+$(50) mixture shows the value of 6×10^{-6} S cm^{-1}. On the other hand, the addition of 50 mol% of **LiTFSI** to **1** increases the conductivity from 1×10^{-8} S cm^{-1} to 4×10^{-6} S cm^{-1} at 100 °C. All the mixtures show a gradual increase in the ionic conductivity with the increase of temperature. Compound **1**/Li$^+$(50) shows a change in the increasing trend of the ionic conductivities between 65 and 80 °C on heating (Fig. 6a), probably due to the slow Cub$_{bi}$–Col$_h$ phase transition.[34,52]

It is noteworthy that the highest conductivities in the **1**/Li$^+$(*x*) and **2**/Li$^+$(*x*) series are obtained in the 1 : 1 mixtures (Fig. 6). Previous studies on LC lithium ion transport materials used lower amounts of lithium salts.[31,55,63,64] Generally, a low lithium ion concentration in the electrolytes leads to better ionic conductivities.[67,68] For example, McFarlane and coworkers reported that for the binary mixtures of *N*-alkyl-methylpyrrolidinium TFSI and **LiTFSI** the conductivity continued to increase by doping less than 30 mol% of **LiTFSI** and further doping up to 50 mol% of **LiTFSI** resulted in the decrease in the conductivity.[68] It is assumed that in the present system the 1 : 1 mixtures form ionic liquid-like structures[62] within the ionic channels, resulting in the increase of the ionic mobility.

Interestingly, the addition of **PC** to **1**/Li$^+$(*x*) and **2**/Li$^+$(*x*) leads to the enhancement of ionic conductivities (Fig. 7 and S12†). The ionic conductivity of **1**/Li$^+$(50) increases four times after the addition of 5 or 10 wt% of **PC** (Fig. 7a). On the other hand, a stepwise increase in the conductivities for **2**/Li$^+$(50) is seen by adding 5 and 10 wt% of **PC** (Fig. 7b). The highest ionic conductivities in the series are observed for **2**/Li$^+$(50)**PC**(10). The value reaches 10^{-4} S cm^{-1} at around 100 °C.‖

The activation energies (E_a) of ion conduction were estimated for **1**/Li$^+$(50) and **1**/Li$^+$(50)**PC**(10) in the Cub$_{bi}$ phases and for **2**/Li$^+$(50) and **2**/Li$^+$(50)**PC**(10) in the Col$_h$ phases (ESI†). It was found that E_a significantly decreased after the addition of **PC** to **1**/Li$^+$(*x*) and **2**/Li$^+$(*x*). For example, the value of E_a for **1**/Li$^+$(50) in the Cub$_{bi}$ phase was 64 kJ mol^{-1}, while that for **1**/Li$^+$(50)**PC**(10) was 41 kJ mol^{-1}. In the case of **2**/Li$^+$(50) and **2**/Li$^+$(50)**PC**(10) in the Col$_h$ phase, the values are 38 kJ mol^{-1} and 23 kJ mol^{-1}, respectively. These reductions in the E_a by the addition of **PC** were attributed to the weakening of the interactions between zwitterions and lithium ions upon the formation of ion–dipole interactions between the lithium ions and **PC** (Fig. 3). The

‖ Thermogravimetric analyses of **PC**-containing mixtures indicate that the evaporation of **PC** under an N_2 flow starts below 100 °C. (Fig. S1). This evaporation is slower when the samples are sandwiched.

formation of more mobile ionic channels would facilitate the transport of lithium ions.

Conclusions

We successfully developed 1D and 3D lithium ion transport LC materials by the co-assembly of wedge-shaped zwitterions (**1** or **2**), **LiTFSI** and **PC**. LC zwitterions provide stable nanostructured media for lithium ion transport and exhibit LC phases with up to 50 mol% of **LiTFSI** and up to 10 wt% of **PC**. The LC phases and ionic conductivities are tuned by the appropriate molecular design and changing the ratio of **LiTFSI** and **PC**. Remarkably, the supramolecular interactions between zwitterions, **LiTFSI** and **PC** are the key for the stabilization of LC phases and for the enhancement of conductivities. It is expected that the ionic conductivities may be further enhanced by increasing the **PC** fraction of the electrolyte materials. The system described here introduces important advances in the development of nanostructured lithium ion-conductive materials, and opens new pathways for the development of LC electrolytes that can be applied in energy devices.

Experimental

Synthesis and characterization of compounds **1** and **2** are described in the ESI.†

Preparation of the mixtures

Compounds **1** and **2** were dried under vacuum at 80 °C for 12 h before their use. They showed no hygroscopic behavior for a period of days under ambient conditions. All the materials and solvents for the preparation of the mixtures were dried before use.

Mixtures **1**/**Li**$^+$(x) and **2**/**Li**$^+$(x) were prepared by adding the appropriate volume of a THF solution of **LiTFSI** (0.026 M) to a weighed amount of zwitterions **1** and **2** (10–30 mg) in a microtube. The solution was homogenised by sonication and then the solvent was slowly removed by rotary evaporation. The samples were dried under vacuum at 80 °C for 12 h before their study. The absence of volatiles was confirmed by thermogravimmetric analyses (Fig. S1†).

The mixtures **1**/**Li**$^+$(x)**PC**(y) and **2**/**Li**$^+$(x)**PC**(y) were prepared by adding the appropriate amount of **PC** to **1**/**Li**$^+$(x) and **2**/**Li**$^+$(x), respectively. The solid blend was homogenised by using a spatula and then heated to 50 °C for 5 min. These mixtures were prepared under ambient conditions in the laboratory (humidity: 40–60 %). The presence of volatiles was monitored by thermogravimetric analyses (Fig. S1†). The thermograms indicate no inclusion of volatiles in the sample, but the loss of less than 1 wt% of the added **PC** during the sample preparation (Fig. S1†).

Acknowledgements

This study was partially supported by the Funding Program for World-Leading Innovative R&D on Science and Technology (FIRST) from the Cabinet Office, Government of Japan. This work was also partially supported by a Grant-in-Aid for Scientific Research (no. 22107003) in the Innovative Area of "Fusion Materials" (Area no. 2206) from the Ministry of Education, Culture, Sports, Science and Technology (MEXT). M. Y. is grateful for financial support from Grant-in-Aid for Young Scientists (A) (no. 2570813) from the Japan Society for the Promotion of Science and The Noguchi Institute.

Notes and references

1 *Handbook of Liquid Crystals*, ed. J. W. Goodby, P. J. Collings, T. Kato, C. Tschierske, H. Gleeson and P. Raynes, Wiley-VCH, Weinheim, Germany, 2nd edn, 2014.
2 T. Kato, N. Mizoshita and K. Kishimoto, *Angew. Chem., Int. Ed.*, 2006, **45**, 38–68.
3 D. J. Broer, C. M. W. Bastiaansen, M. G. Debije and A. P. H. J. Schenning, *Angew. Chem., Int. Ed.*, 2012, **51**, 7102–7109.
4 W. Pisula, X. Feng and K. Müllen, *Adv. Mater.*, 2010, **22**, 3634–3649.
5 N. Houbenov, J. S. Haataja, H. Iatrou, N. Hadjichristidis, J. Ruokolainen, C. F. J. Faul and O. Ikkala, *Angew. Chem., Int. Ed.*, 2011, **50**, 2516–2520.
6 B. M. Rosen, C. J. Wilson, D. A. Wilson, M. Peterca, M. R. Imam and V. Percec, *Chem. Rev.*, 2009, **109**, 6275–6540.
7 T. Kato, *Science*, 2002, **295**, 2414–2418.
8 S. Chen and S. H. Eichhorn, *Isr. J. Chem.*, 2012, **52**, 830–843.
9 C. F. J. Faul and M. Antonietti, *Adv. Mater.*, 2003, **15**, 673–683.
10 B. R. Wiesenauer and D. L. Gin, *Polym. J.*, 2012, **44**, 461–468.
11 D. L. Gin, C. S. Pecinovsky, J. E. Bara and R. L. Kerr, *Struct. Bonding*, 2008, **128**, 181–222.
12 M. Funahashi, H. Shimura, M. Yoshio and T. Kato, *Struct. Bonding*, 2008, **128**, 151–180.
13 S. Sergeyev, W. Pisula and Y. H. Geerts, *Chem. Soc. Rev.*, 2007, **36**, 1902–1929.
14 K. Binnemans, *Chem. Rev.*, 2005, **105**, 4148–4204.
15 T. Kato, *Angew. Chem., Int. Ed.*, 2010, **49**, 7847–7848.
16 I. M. Saez and R. J. W. Goodby, *Struct. Bonding*, 2008, **128**, 1–62.
17 C. Tschierske, *Chem. Soc. Rev.*, 2007, **36**, 1930–1970.
18 B. Donnio, S. Buathong, I. Bury and D. Guillon, *Chem. Soc. Rev.*, 2007, **36**, 1495–1513.
19 M. Marcos, R. Martın-Rapún, A. Omenat and J. L. Serrano, *Chem. Soc. Rev.*, 2007, **36**, 1889–1901.
20 M. Yoshio and T. Kato, in *Handbook of Liquid Crystals*, ed. J. W. Goodby, P. J. Collings, T. Kato, C. Tschierske, H. Gleeson and P. Raynes, Wiley-VCH, Weinheim, 2nd edn, 2014, vol. 8, ch. 23, pp. 727–749.
21 C. F. Van Nostrum and R. J. M. Nolte, *Chem. Commun.*, 1996, 2385–2392.
22 Y. G. Zheng, J. G. Liu, Y. P. Liao, G. Ungar and P. V. Wright, *Dalton Trans.*, 2004, 3053–3060.
23 U. Beginn, G. Zipp and M. Moller, *Adv. Mater.*, 2000, **12**, 510–511.
24 N. Sakai and S. Matile, *Langmuir*, 2013, **29**, 9031–9040.
25 M. Armand and J. M. Tarascon, *Nature*, 2008, **451**, 652–657.

26 Y. B. Chen, M. Thorn, S. Christensen, C. Versek, A. Poe, R. C. Hayward, M. T. Tuominen and S. Thayumanavan, *Nat. Chem.*, 2010, **2**, 503–508.
27 Y. Kim, W. Li, S. Shin and M. Lee, *Acc. Chem. Res.*, 2013, **46**, 2888–2897.
28 B.-K. Cho, A. Jain, S. M. Gruner and U. Wiesner, *Science*, 2004, **305**, 1598–1601.
29 H.-K. Lee, H. Lee, Y. H. Ko, Y. J. Chang, N.-K. Oh, W.-C. Zin and K. Kim, *Angew. Chem., Int. Ed.*, 2001, **40**, 2669–2671.
30 V. Percec, G. Johansson, J. Heck, G. Ungar and S. V. Batty, *J. Chem. Soc., Perkin Trans. 1*, 1993, 1411–1420.
31 R. L. Kerr, S. A. Miller, R. K. Shoemaker, B. J. Elliott and D. L. Gin, *J. Am. Chem. Soc.*, 2009, **131**, 15972.
32 M. Yoshio, T. Mukai, K. Kanie, M. Yoshizawa, H. Ohno and T. Kato, *Adv. Mater.*, 2002, **14**, 351–354.
33 M. Yoshio, T. Mukai, H. Ohno and T. Kato, *J. Am. Chem. Soc.*, 2004, **126**, 994–995.
34 T. Ichikawa, M. Yoshio, A. Hamasaki, T. Mukai, H. Ohno and T. Kato, *J. Am. Chem. Soc.*, 2007, **129**, 10662–10663.
35 M. Yoshio, T. Ichikawa, H. Shimura, T. Kagata, A. Hamasaki, T. Mukai, H. Ohno and T. Kato, *Bull. Chem. Soc. Jpn.*, 2007, **80**, 1836–1841.
36 T. Ohtake, M. Ogasawara, K. Ito-Akita, N. Nishina, S. Ujiie, H. Ohno and T. Kato, *Chem. Mater.*, 2000, **12**, 782–789.
37 P. H. J. Kouwer and T. M. Swager, *J. Am. Chem. Soc.*, 2007, **129**, 14042–14052.
38 B.-K. Cho, *RSC Adv.*, 2014, **4**, 395–405.
39 K. Kishimoto, M. Yoshio, T. Mukai, M. Yoshizawa, H. Ohno and T. Kato, *J. Am. Chem. Soc.*, 2003, **125**, 3196–3197.
40 H. Shimura, M. Yoshio, A. Hamasaki, T. Mukai, H. Ohno and T. Kato, *Adv. Mater.*, 2009, **21**, 1591–1594.
41 X. Feng, M. E. Tousley, M. G. Cowan, B. R. Wiesenauer, S. Nejati, Y. Choo, R. D. Noble, M. Elimelech, D. L. Gin and C. O. Osuji, *ACS Nano*, 2014, **8**, 11977–11986.
42 B. Soberats, E. Uchida, M. Yoshio, J. Kagimoto, H. Ohno and T. Kato, *J. Am. Chem. Soc.*, 2014, **136**, 9552–9555.
43 A. Yamashita, M. Yoshio, S. Shimizu, T. Ichikawa, H. Ohno and T. Kato, *J. Polym. Sci., Part A: Polym. Chem.*, 2015, **53**, 366–371.
44 T. Ichikawa, M. Yoshio, A. Hamasaki, S. Taguchi, F. Liu, X. B. Zeng, G. Ungar, H. Ohno and T. Kato, *J. Am. Chem. Soc.*, 2012, **134**, 2634–2643.
45 S. Kutsumizu, *Isr. J. Chem.*, 2012, **52**, 844–853.
46 E. S. Hatakeyama, B. R. Wiesenauer, C. J. Gabriel, R. D. Noble and D. L. Gin, *Chem. Mater.*, 2010, **22**, 4525–4527.
47 D. Högberg, B. Soberats, S. Uchida, L. Kloo, H. Segawa and T. Kato, *Chem. Mater.*, 2014, **26**, 6496–6502.
48 J. Sakuda, E. Hosono, M. Yoshio, T. Ichikawa, T. Matsumoto, H. Ohno, H. Zhou and T. Kato, *Adv. Funct. Mater.*, 2015, **25**, 1206–1212.
49 R. D. Costa, F. Werner, X. J. Wang, P. Gronninger, S. Feihl, F. T. U. Kohler, P. Wasserscheid, S. Hibler, R. Beranek, K. Meyer and D. M. Guldi, *Adv. Energy Mater.*, 2013, **3**, 657–665.
50 N. Yamanaka, R. Kawano, W. Kubo, N. Masaki, T. Kitamura, Y. Wada, M. Watanabe and S. Yanagida, *J. Phys. Chem. B*, 2007, **111**, 4763–4769.
51 T. Ichikawa, M. Yoshio, S. Taguchi, J. Kagimoto, H. Ohno and T. Kato, *Chem. Sci.*, 2012, **3**, 2001–2008.
52 B. Soberats, M. Yoshio, T. Ichikawa, S. Taguchi, H. Ohno and T. Kato, *J. Am. Chem. Soc.*, 2013, **135**, 15286–15289.
53 T. Ichikawa, T. Kato and H. Ohno, *J. Am. Chem. Soc.*, 2012, **134**, 11354–11357.
54 T. Matsumoto, T. Ichikawa, J. Sakuda, T. Kato and H. Ohno, *Bull. Chem. Soc. Jpn.*, 2014, **87**, 792–796.
55 T. Ichikawa, M. Yoshio, A. Hamasaki, J. Kagimoto, H. Ohno and T. Kato, *J. Am. Chem. Soc.*, 2011, **133**, 2163–2169.
56 W. J. Middleton and V. A. Engelhardt, *J. Am. Chem. Soc.*, 1958, **80**, 2788–2794.
57 M.-L. Pujol-Fortin and J.-C. Galin, *Macromolecules*, 1991, **24**, 4523–4530.
58 M. Galin, A. Chapoton and J. C. Galin, *J. Chem. Soc., Perkin Trans. 2*, 1993, 545–553.
59 A. Mathis, M. Galin, J. C. Galin, B. Heinrich and C. G. Bazuin, *Liq. Cryst.*, 1999, **26**, 973–984.
60 S. Ueda, J. Kagimoto, T. Ichikawa, T. Kato and H. Ohno, *Adv. Mater.*, 2011, **23**, 3071–3074.
61 K. Xu, *Chem. Rev.*, 2004, **104**, 4303–4417.
62 M. Yoshizawa, A. Narita and H. Ohno, *Aust. J. Chem.*, 2004, **57**, 139–144.
63 J. C. Y. Lin, C.-J. Huang, Y.-T. Lee, K.-M. Lee and I. J. B. Lin, *J. Mater. Chem.*, 2011, **21**, 8110–8121.
64 R. Rondla, J. C. Y. Lin, C. T. Yang and I. J. B. Lin, *Langmuir*, 2013, **29**, 11779–11785.
65 M. Yoshizawa, M. Hirao, K. Ito-Akita and H. Ohno, *J. Mater. Chem.*, 2001, **11**, 1057–1062.
66 H. Lee, D. B. Kim, S.-H. Kim, H. S. Kim, S. J. Kim, D. K. Choi, Y. S. Kang and J. Won, *Angew. Chem., Int. Ed.*, 2004, **43**, 3053–3056.
67 S. Sylla, J.-Y. Sanchez and M. Armand, *Electrochim. Acta*, 1992, **37**, 1699–1701.
68 D. R. MacFarlane, J. Huang and M. Forsyth, *Nature*, 1999, **402**, 792–794.

